Inorganic Chemistry
Article

Inorg. Chem. **2011**, *50*, 949–955 **949**
DOI: 10.1021/ic101538v

Assembly of a Trifunctional Artificial Peptide Into an Anti-Parallel Duplex with Three Cu(II) Cross-links

Matthew B. Coppock, James R. Miller, and Mary Elizabeth Williams*

Department of Chemistry, The Pennsylvania State University, 104 Chemistry Building, University Park, Pennsylvania 16802, United States

Received July 30, 2010

Analogous to self-assembly in natural DNA or proteins, we describe the synthesis of a heterofunctional artificial tripeptide that self-assembles into an antiparallel duplex by coordination of three Cu(II) ions. The tripeptide contains three pendant ligands, pyridine (py), methyl bipyridine (bpy), and terpyridine (tpy), in series on an aminoethylglycine (aeg) backbone. These ligands chelate three Cu(II) ions, forming two $[Cu(tpy)(py)]^{2+}$ and one $[Cu(bpy)_2]^{2+}$ complexes, that cross-link two tripeptide strands to give a trimetallic supramolecular structure. The tripeptide and metal-linked tripeptide duplex are characterized with NMR spectroscopy, mass spectrometry, and analytical high performance liquid chromatography (HPLC). Spectrophotometric titrations are used to quantitatively examine the stoichiometry of binding. Together with electron paramagnetic resonance (EPR) spectroscopy, the identities of the Cu(II) complexes and their environments are examined. The EPR spectrum reveals a significant amount of coupling between metal centers compared to a dimetallic dipeptide analogue. EPR and UV−vis absorbance spectroscopy, together with molecular modeling, provide evidence that the tripeptide acts as a scaffold to hold the metal centers in close proximity.

Introduction

The control of the geometries and spacing of functional complexes is an important aspect in the design of inorganic supramolecular structures. Molecular recognition and self-assembly, such as in DNA and proteins, are approaches commonly used to create complex synthetic molecular architectures. Substitution of nucleobases in DNA,[1] PNA,[2] and GNA[3] with redox active inorganic complexes has been described as a method for preparing functional self-assembled structures. However, nucleic acids' irreversible redox chemistry[4] and affinity for metal ions[5] place limits on their utility for some of their potential applications as molecular wires and barcodes, sensors, and artificial enzymes.

Our approach has been to direct self-assembly of polymetallic supramolecular structures with artificial peptides because these are charge neutral and redox inactive. We have initially focused on the synthesis of homofunctional oligopeptides containing solely pendant bpy or phenyl tpy ligands.[6a,b] More recently we have sought to exert better control over structural arrangement by preventing strand misalignment and parallel/antiparallel isomer formation in the duplexes.[6c−e] We recently reported the synthesis of two "self-complementary" heterofunctional dipeptides (Figure 1A): these are designed to create double-stranded duplexes cross-linked by two $[Cu(tpy)(py)]^{2+}$ complexes, yielding an antiparallel strand alignment.[6d] We predict that as the length of the oligopeptide increases, the resulting metal-linked duplex should become more rigid, giving rise to stronger electronic interactions between adjacent metal centers. To maintain the self-complementary motif in Figure 1A and lengthen the strand, incorporation of an additional functional group is necessary (Figure 1B). Inserting a third type of ligand further has the potential to introduce increasing electronic complexity, observed as changes in the spectroscopy, electrochemistry, and so forth.

Herein we describe a self-complementary hetero-trifunctional oligopeptide that is designed to form antiparallel duplexes upon coordination of three Cu(II) ions (Figure 1B).

*To whom correspondence should be addressed. E-mail: mbw@chem.psu.edu.

(1) (a) Meggers, E.; Holland, P. L.; Tolman, W. B.; Romesberg, F. E.; Schultz, P. G. *J. Am. Chem. Soc.* **2000**, *122*, 10714–10715. (b) Atwell, S.; Meggers, E.; Spraggon, G.; Schultz, P. G. *J. Am. Chem. Soc.* **2001**, *123*, 12364–12367. (c) Tanaka, K.; Tengeiji, A.; Kato, T.; Toyama, N.; Shionoya, M. *Science* **2003**, *299*, 1212–1213.

(2) (a) Popescu, D.-L.; Parolin, T. J.; Achim, C. *J. Am. Chem. Soc.* **2003**, *125*, 6354–6355. (b) Watson, R. M.; Skorik, Y. A.; Patra, G. K.; Achim, C. *J. Am. Chem. Soc.* **2005**, *127*, 14628–14639. (c) Franzini, R. M.; Watson, R. M.; Patra, G. K.; Breece, R. M.; Tierney, D. L.; Hendrich, M. P.; Achim, C. *Inorg. Chem.* **2006**, *45*, 9798–9811.

(3) (a) Schlegel, M. K.; Zhang, L.; Pagano, N.; Meggers, E. *Org. Biomol. Chem.* **2009**, *7*, 476–482. (b) Schlegel, M. K.; Essen, L.-O.; Meggers, E. *J. Am. Chem. Soc.* **2008**, *130*, 8158–8159.

(4) Paleek, E. *Talanta* **2002**, *56*, 809–819.

(5) (a) Katz, S. *Biochim. Biophys. Acta* **1963**, *68*, 240–253. (b) Lee, J. S.; Latimer, L. J. P.; Reid, R. S. *Biochem. Cell Biol.* **1993**, *71*, 162–168.

Published on Web 01/06/2011

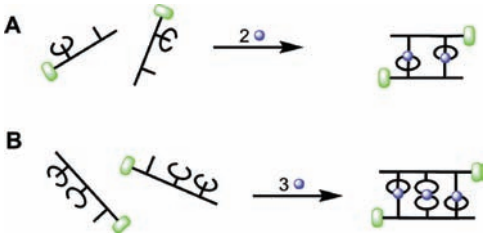

Figure 1. Antiparallel self-assembling scheme of pendant (A) monodentate-tridentate and (B) monodentate-bidentate-tridentate ligands in series on an aeg backbone because of the addition of a tetracoordinate metal (blue circles).

We utilize this structure to demonstrate the methodology for making longer and more complex architectures, and for testing the hypothesis that longer sequences provide additional rigidity and metal−metal interactions. The tripeptide was synthesized to contain tethered monodentate py, bidentate bpy, and tridentate tpy ligands in series on an aeg backbone (Scheme 1). In the presence of Cu(II), possible complexes are $[Cu(tpy)(py)]^{2+}$,[6d] $[Cu(bpy)_2]^{2+}$,[7] $[Cu(tpy)_2]^{2+}$,[8] $[Cu(tpy)(bpy)]^{2+}$, $[Cu(bpy)(py)]^{2+}$, and $[Cu(bpy)(py)_2]^{2+}$.[9] Although the oligopeptide is flexible, the distance between the ligands on the backbone is not sufficient for adjacent sites on the chain to coordinate to the same metal ion. Formation of these complexes would form coordinative cross-links between oligopeptide strands; however, only formation of solely $[Cu(tpy)(py)]^{2+}$ and $[Cu(bpy)_2]^{2+}$ complexes would yield a product with three metal ions and two antiparallel tripeptide strands. It has been shown previously that metal coordination based self-assembly into closed cycles is a thermodynamically driven, dynamic process whereby components assemble and disassemble until the most exergonically favorable configuration is obtained.[10] We hypothesize that the lability of Cu(II) enables the entropically favored tripeptide duplex to form in a fashion similar to the previously described dipeptides.[6d] Therefore, in this paper we examine the binding of Cu(II) to the heterotrifunctional oligopeptide and compare the properties of the resulting structure to the shorter Cu-linked dipeptide duplex in efforts to improve and understand oligopeptide-directed self-assembly of multimetallic architectures.

Experimental Section

Instrumentation and Analysis. Positive-ion electrospray mass spectrometry (ESI+) was performed at the Penn State Mass Spectrometry Facility using a Mariner mass spectrometer (Perseptive Biosystems). All NMR spectra were collected on 300, 360, or 400 MHz spectrometers (Bruker). Solution molecular weights were estimated using a Wespro Vapro model 5520 vapor pressure osmometer using 10−25 mmol/kg solutions in acetonitrile (ACN). A standard calibration curve was obtained using solutions of known concentration of tetrabutylammonium perchlorate in ACN. The UV−vis absorbance spectra were obtained using a double-beam spectrophotometer (Varian, Cary 500) and background subtracted using the reference cell of the double-beam spectrophotometer. X-band EPR spectra were obtained using a 9.51 GHz Bruker eleXsys 500 spectrometer equipped with a liquid helium cryostat; all experiments were performed at 12 K with a modulation frequency of 100 kHz, modulation amplitude of 5 G, and a microwave power of 0.1 μW. Cu(II) concentrations were experimentally determined using a Cu(II) standard.

Analytical-scale high performance liquid chromatography (HPLC) was performed with a Varian system equipped with two quaternary pumps (Model 210), an autosampler (Model 410), a UV−vis detector (Model 320), and a Thermo Scientific Betasil Silica-100 column (150 mm ×4.6 mm with 5 μm particle size). The tripeptide and its Cu(II)-containing product (2.0 μL injections) were separately analyzed using a flow rate of 0.5 mL/min. The eluent contained 0.1% trifluoroacetic acid (TFA) in a mixture of acetonitrile (ACN), water, and saturated aqueous potassium nitrate in a 6:3:1 volume ratio, respectively. Elution of the compounds was monitored at 300 nm.

Chemicals. All chemicals were reagent grade and used as received unless otherwise noted. N-Hydroxybenzotriazole (HOBt) and 1-ethyl-3-(3-dimethylaminopropyl)carbodiimide hydrochloride (EDC) were purchased from Advanced ChemTech. O-Benzotriazole-*N*,*N*,*N*′,*N*′-tetramethyl-uronium-hexafluorophosphate (HBTU) was purchased from NovaBiochem. All other chemicals were purchased from Aldrich. 4′-Methyl-2,2′-bipyridine-4-acetic acid,[11] Fmoc-aeg-O*t*Bu·HCl,[12] Fmoc-aeg(py)−OH·HCl,[6a] Fmoc-aeg(bpy)-O*t*Bu,[6b] 4′-Methyl-2,2′:6′,2″-terpyridine,[13] pyridacyl pyridinium iodide,[14] 4′-acetic acid-2,2′:6′,2″-terpyridine,[6d] Fmoc-aeg(tpy)-O*t*Bu,[6d] Fmoc-aeg(py)-aeg(tpy)-O*t*Bu,[6d] Aquo(2,2′,2″-terpyridine)copper(II) Diperchlorate,[8] and Pyridine(2,2′,2″-terpyridine)copper(II) Diperchlorate[8] were synthesized, isolated, and characterized as previously reported. Water was purified using a Nanopure water system (Barnstead, 18.2 MΩ). Fmoc deprotection and terminal acid formation were performed using previously published methods.[6d]

Synthesis. A. Fmoc-aeg(py)-aeg(bpy)-O*t*Bu (1). Fmoc-aeg(py)−OH·HCl (1.36 g, 2.7 mmol), HBTU (1.04 g, 2.7 mmol), HOBt (0.37 g, 2.7 mmol), and DIPEA (2.1 mL, 12 mol) were combined in DCM (100 mL) and stirred for 15 min at 0 °C. The mixture was added to aeg(bpy)-O*t*Bu (0.70 g, 1.8 mmol) dissolved in DCM (25 mL) and stirred at 25 °C for 48 h. The solution was extracted with water (3 × 25 mL) and back extracted with DCM (25 mL). The organics were dried over Na_2SO_4, the solids removed, and the solvent was flash evaporated to yield a yellow oil. The oil was purified on a silica gel column, eluted with a solvent gradient (100% DCM to 5% MeOH in DCM), and yellow fractions were dried to give a pale yellow solid. Yield = 0.500 g (33%). ^{1}H NMR (360 MHz, chloroform-d): δ 8.61−8.50 (m, 2H); 8.41(m, 2H); 8.28−8.16 (m, 2H); 7.73 (d, J = 7 Hz, 2H); 7.59 (t, J = 7 Hz, 2H); 7.37 (t, J = 7 Hz, 2H); 7.27 (m, 3H); 7.19−7.12 (m, 3H); 4.40−4.25 (d, J = 6 Hz, 2H); 4.25−4.15 (t, J = 4 Hz, 1H); 4.07−3.86 (m, 4H);

(6) (a) Gilmartin, B. P.; Ohr, K.; McLaughlin, R. L.; Koerner, R.; Williams, M. E. *J. Am. Chem. Soc.* **2005**, *127*, 9546–9555. (b) Ohr, K.; McLaughlin, R. L.; Williams, M. E. *Inorg. Chem.* **2007**, *46*, 965–974. (c) Myers, C. P.; Gilmartin, B. P.; Williams, M. E. *Inorg. Chem.* **2008**, *47*, 6738–6747. (d) Coppock, M. B.; Kapelewski, M. T.; Youm, H. W.; Levine, L. A.; Miller, J. R.; Myers, C. P.; Williams, M. E. *Inorg. Chem.* **2010**, *49*, 5126–5133. (e) Myers, C. P.; Miller, J. R.; Williams, M. E. *J. Am. Chem. Soc.* **2009**, *42*, 15291–15300.
(7) Garribba, E.; Micera, G.; Sanna, D.; Strinna-Erre, L. *Inorg. Chim. Acta* **2000**, *299*, 253–261.
(8) Harris, C. M.; Lockyer, T. N. *Aust. J. Chem.* **1970**, *23*, 673–682.
(9) Arena, G.; Bonomo, R. P.; Musumeci, S.; Purrello, R.; Rizzarelli, E. *J. Chem. Soc., Dalton Trans.* **1983**, 1279–1283.
(10) (a) Northrop, B. H.; Hai-bo, Y.; Stang, P. J. *Chem. Commun.* (*Camb*) **2008**, *45*, 5896–5908. (b) Sun, W.-Y.; Yoshizawa, M.; Kusukawa, T.; Fujita, M. *Curr. Opin. Cell. Biol.* **2002**, *6*, 757–764.
(11) Ciana, L. D.; Hamachi, I.; Meyer, T. J. *J. Org. Chem.* **1989**, *54*, 1731–1735.
(12) Thomson, S. A.; Josey, J. A.; Cadilla, R.; Gaul, M. D.; Hassman, C. F.; Luzzio, M. J.; Pipe, A. J.; Reed, K. L.; Ricca, D. J.; Wiethe, R. W.; Noble, S. A. *Tetrahedron* **1995**, *51*, 6179–6194.
(13) Wolpher, H.; Sinha, S.; Pan, J.; Johansson, A.; Lundqvist, M. J.; Persson, P.; Lomoth, R.; Bergquist, J.; Sun, L.; Sundstrom, V.; Akermark, B.; Polivka, T. *Inorg. Chem.* **2007**, *46*, 638–651.
(14) Priimov, G. U.; Moore, P.; Maritim, P. K.; Butalanyi, P. K.; Alcock, N. W. *J. Chem. Soc., Dalton Trans.* **2000**, 445–449.

Scheme 1. Synthesis of Tripeptide[a]

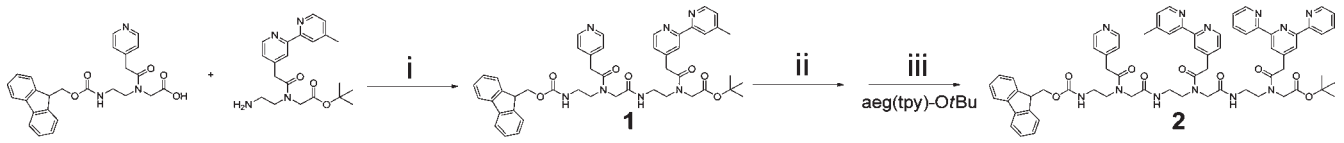

[a] (i) HBTU, HOBt, DIPEA, η: 33%; (ii) 1:1 TFA:DCM, η: 80%; (iii) EDC, HOBt, DIPEA, η: 21%.

3.77−3.67 (m, 4H); 3.63−3.48 (m, 4H); 3.46−3.30 (m, 4H); 2.42 (s, 3H); 1.44 (m, 9H). MS (ESI+) $[M + H]^+$ calcd 825.95, found 826.4.

B. Fmoc-aeg(py)-aeg(bpy)-aeg(tpy)-O*t*Bu (2). A solution of Fmoc-aeg(py)-aeg(bpy)−OH (0.400 g, 0.52 mmol), EDC (0.010 g, 0.52 mmol), HOBt (0.070 g, 0.52 mmol), and DIPEA (0.26 mL, 1.6 mmol) in DCM (40 mL) was stirred at 0 °C for 15 min. The mixture was added to aeg(tpy)-O*t*Bu (0.18 g, 0.40 mmol) dissolved in DCM (10 mL) and stirred at 25 °C for 48 h. The solution was extracted with water (3 × 20 mL) and back extracted with DCM (20 mL). The organics were dried over Na_2SO_4, and the solvent was removed via flash evaporation, giving a yellow solid. The solid was purified on a silica column with a solvent gradient (100% DCM to 30% MeOH in DCM), a pale yellow band was collected and dried to give a yellow solid. Yield = 0.100 g (21%). ^{1}H NMR (400 MHz, chloroform-d): δ 8.62−8.60 (m, 4H); 8.54−8.52 (m, 1H); 8.45−8.42 (m, 3H); 8.30 (s, 1H); 8.25 (s, 1H); 8.16−8.12 (m, 2H); 7.81 (m, 2H); 7.70 (m, 2H); 7.54 (t, J = 7 Hz, 2H); 7.34 (m, 2H); 7.30−7.22 (m, 4H); 7.13 (m, 1H); 7.06 (m, 2H); 6.99 (m, 1H); 4.35−4.20 (m, 2H); 4.17−4.10 (m, 1H); 4.07−3.82 (m, 6H); 3.80−3.63 (m, 6H); 3.60−3.37 (m, 6H); 3.36−3.05 (m, 6H); 2.38 (s, 3H); 1.43 (m, 9H). HR MS (ESI+) $[M + H]^+$ calcd 1199.5467, found 1199.5448. Elemental Analysis. **Fmoc-aeg(py)-aeg(bpy)-aeg(tpy)-O*t*Bu·H_2O·CH_2Cl_2** Calc: 63.64 C; 5.73 H; 12.91 N; Found: 64.08 C; 5.68 H; 12.92 N.

Reaction with Cu(II). A solution of tripeptide **2** was dissolved in methanol and combined with 1.5 equiv of $Cu(NO_3)_2 \cdot 2.5$ H_2O, stirred, and heated at 40 °C for 24 h. The solvent was removed under reduced pressure, and the residue was dissolved in 10 mL of 1:4 methanol/water. A saturated aqueous solution of NH_4PF_6 was added, immediately producing a light blue colored precipitate. The solid was collected by filtration and rinsed with methanol and ether. $[Cu_3(\mathbf{2})_2](PF_6)_x(NO_3)_y$ MS (Figure 3) (ESI^+): $[[Cu_3(\mathbf{2})_2](PF_6)_3(NO_3)]^{2+}$ calcd 1542.9, found 1542.7; $[[Cu_3(\mathbf{2})_2](PF_6)_2(NO_3)]^{3+}$ calcd 980.3, found 980.2; $[[Cu_3(\mathbf{2})_2](PF_6)(NO_3)]^{4+}$ calcd 699.0, found 698.9; $[[Cu_3(\mathbf{2})_2](NO_3)]^{5+}$ calcd 530.2, found 530.1. ^{1}H NMR (Supporting Information, Figure S7) (400 MHz, ACN-d_3): δ 7.90−7.25 (br m, 16H); 4.70−2.60 (br m, 54H); 1.35 (br s, 18H).

Spectrophotometric Titrations. Titrations were performed using solutions of tripeptide and $Cu(NO_3)_2$ in methanol; concentration of the tripeptide solution was quantitatively determined using the (separately determined) extinction coefficient. For measurements of visible wavelength absorbance, ∼ 1 mM peptide solutions were used; in the UV region solutions of ∼5 μM peptide were used. Titrations either incrementally added metal to peptide or peptide to metal, as indicated below. Solutions were stirred for 10 min prior to measurement of the absorbance spectrum.

Results and Discussion

Synthesis and Characterization of the Tripeptide. As part of our efforts to examine interactions and electron transfers between metal centers linked within an artificial oligopeptide scaffold,[6] the length of the self-complementary single strand has been extended to three monomer units to create larger multimetallic structures. Following the self-aligning oligopeptide design strategy, a tripeptide is designed similar to the dipeptides but with a bidentate methyl bipyridine monomer unit inserted between monodentate pyridine and tridentate terpyridine ligands.[6d] The synthesis of the tripeptide employs a scheme and conditions that are similar to the previously described dipeptides.[6d] Using Fmoc and *tert*-butyl protection of the aeg backbone termini, the selective deprotection products[6] of the monomers Fmoc-aeg(py)-O*t*Bu, Fmoc-aeg(bpy)-O*t*Bu, and Fmoc-aeg(tpy)-O*t*Bu were reacted to synthesize the target artificial oligopeptide. Scheme 1 shows the stepwise method for making the tripeptide. Dipeptide **1** was synthesized by coupling the amine terminus of the bpy monomer to the acid terminus of the py monomer with HBTU, HOBt, and DIPEA. Following isolation and purification of the dipeptide, the acid terminus was deprotected with TFA and reacted with the amine terminus of the tpy monomer using EDC, HOBt, and DIPEA to give tripeptide **2** in 21% yield. Tripeptide **2** was purified by column chromatography, and analyzed by analytical HPLC and elemental analysis. The chromatogram of the tripeptide (shown in Figure 2) contains a sharp peak at 4.18 min and small peaks of minor intensity (∼ 3.7, 3.9, and 4.6 min); these latter features collectively represent ∼10% of the sample. Because elemental analysis separately verified the purity of the tripeptide, the small peaks in the chromatogram may be a result of aggregation of the neutral tripeptide in the polar conditions of this separation. High resolution electrospray ionization mass spectrometry was used to identify the product by evaluation of the molecular ion peak with respect to the theoretical mass/charge ratio for the tripeptide ($[M+H]^+$ m/z: calculated 1199.5467 m/z, found 1199.5448 m/z).

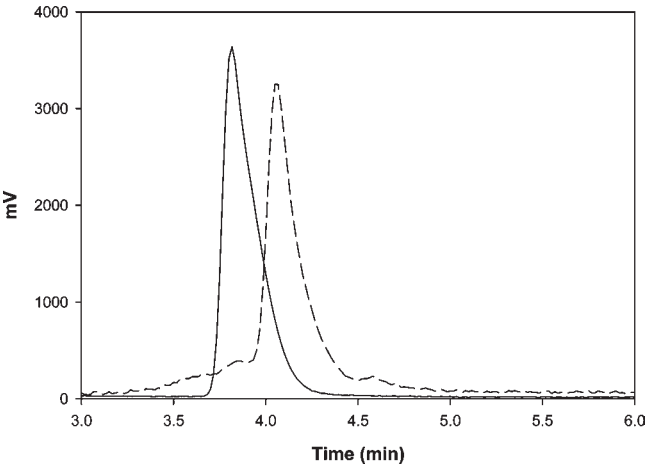

Figure 2. High performance liquid chromatograms using a silica column (150 mm ×4.6 mm with 5 μm particle size) and 6:3:1 mixture of $ACN/H_2O/KNO_3$ with 0.1% TFA, a flow rate of 0.5 mL/min, and monitoring absorbance at 300 nm. Injection volume is 2 μL of ∼1 mg/mL $[Cu_3(\mathbf{2})_2]^{6+}$ (solid line) versus **2** (dashed line).

Integration of the peaks in the ^{1}H NMR spectrum of **2** enables comparison of the aromatic and aliphatic regions as an initial confirmation of purity. In the spectrum of tripeptide **2**, the observed proton integrations 28 aromatic, 27 aliphatic, 3 methyl, and 9 *tert*-butyl protons are consistent with the tripeptide structure as shown in Scheme 1. The fully assigned ^{1}H NMR spectrum of dipeptide **1** (Supporting Information, Figure S1) and assigned 1-D and 2-D spectra for the previously reported Fmoc-aeg(py)-aeg(tpy)-O*t*Bu dipeptide aid in the interpretation of the tripeptide **2** spectra since the proton resonances in the aromatic region appear at similar chemical shifts (Supporting Information, Figures S1−S6).

Analysis of the ^{1}H−^{1}H COSY spectrum of **2** (Supporting Information, Figure S4) shows coupling between neighboring protons on each ligand as well as between protons on the aeg backbone. The py ligand is identified through the coupling of the two protons at 7.06 ppm (Supporting Information, Figure S2, peak l) with the two protons at 8.44 ppm (Supporting Information, Figure S2, peak k). The tpy protons that are adjacent to the nitrogens appear at 8.61 ppm (Supporting Information, Figure S2, peak x) and couple with neighboring protons at 7.26 ppm (Supporting Information, Figure S2, peak w), allowing recognition of the other correlations between tpy protons in the COSY spectrum. Remaining correlations between protons at 6.99 ppm (Supporting Information, Figure S2, peak p) and 8.39 ppm (Supporting Information, Figure S2, peak q), in addition to the protons at 7.13 ppm (Supporting Information, Figure S2, peak s) and 8.53 ppm (Supporting Information, Figure S2, peak r), are attributed to coupling of between protons on the bpy ligand. While other protons at 8.14 ppm (Supporting Information, Figure S2, peak n) and 8.26 ppm (Supporting Information, Figure S2, peak m) have been ascribed to bpy, and the protons at 8.30 ppm (Supporting Information, Figure S2, peak t) belong to tpy, none show coupling in the COSY spectrum since they are electronically isolated. Additional couplings between protons on the Fmoc protecting group (7.31−7.75 ppm and 4.10−4.40 ppm, Supporting Information, Figure S2 peaks a−f) and the aeg backbone (3.15−4.00 ppm, Supporting Information, Figure S2 peaks g−j) are also observed. These data, together with the ^{13}C−^{1}H HMQC (Supporting Information, Figure S5), ^{13}C−^{1}H HMBC (Supporting Information, Figure S6) spectra, and mass spectrometry, confirm the identity of the tripeptide, and purity is affirmed using HPLC and elemental analysis.

Synthesis of Cu(II) Complex. Addition of Cu(II) to the tripeptide is expected to result in coordination to the ligands pendant on the oligopeptide, and when possible, do so in such a way as to achieve coordinative saturation. With three different ligands on the aeg scaffold, there are many possible Cu(II) complexes that can form (vide supra) among which are included [Cu(tpy)(py)]$^{2+}$[6d] and [Cu(bpy)$_2$]$^{2+}$.[7] To investigate oligopeptide-directed assembly of multimetallic structures, the tripeptide was therefore reacted with Cu(II). The resulting light blue product was isolated by precipitation with ammonium hexafluorophosphate, and analytical HPLC was used to confirm the purity of the product. Figure 2 shows that under identical conditions, the Cu(II) complex elutes in a shorter amount of time than the pure (unmetalated) tripeptide. With this mobile phase, earlier elution is indicative of higher ionic charge in solution. In the chromatogram of the Cu(II) complex, the presence of a single peak confirms the purity of a single Cu(II)-containing product. Vapor pressure osmometry (VPO) was employed to gauge the average molecular weight of the copper complex in an acetonitrile solution. Using calibration curves that we have previously employed,[6d] an average molecular weight of 4.1×10^3 g/mol was determined; this value is consistent with a metal complex containing three copper centers bound to two tripeptides.

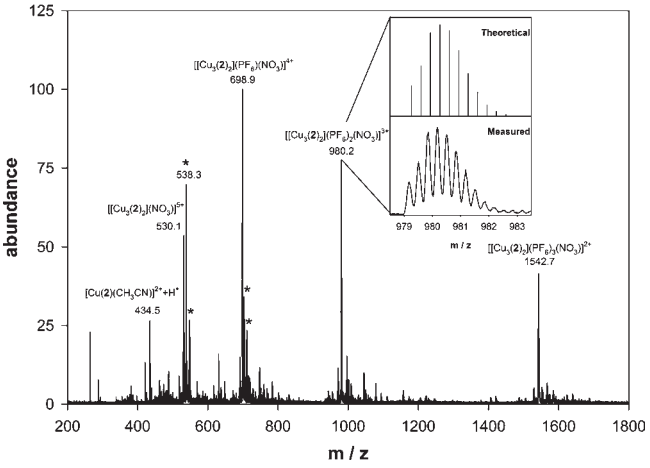

Figure 3. Positive ion electrospray mass spectrum of $[Cu_3(\mathbf{2})_2]^{6+}$, which is observed together with associated PF_6^- and NO_3^- anions as indicated. The inset is the theoretical and observed isotope patterns for the +3 charged ion $[Cu_3(\mathbf{2})_2(PF_6)_2\ (NO_3)]^{3+}$. Asterisks (*) indicate a fragment with at least one associated CH_3CN molecule.

To identify the Cu(II)-tripeptide product, ESI+ mass spectrometry was used. Figure 3 contains the mass spectrum that was acquired under sufficiently mild ionization conditions such that multiple molecular ion peaks are observed, similar to previously published results.[6d] A base molecular ion peak is observed at 698.9 *m*/*z* for a +4 charge species; by comparison with the theoretical isotopic splitting patterns of possible products, this peak is attributed to the product $[[Cu_3(\mathbf{2})_2](PF_6)(NO_3)]^{4+}$. An example of the excellent agreement between theoretical and experimental peaks is shown in the Figure 3 inset for a +3 charged species. Similar analysis of additional major peaks in the mass spectrum shows that these are due to the molecular ion $[Cu_3(\mathbf{2})_2]^{6+}$ associated with varying numbers of anions: $[[Cu_3(\mathbf{2})_2](PF_6)_3(NO_3)]^{2+}$, $[[Cu_3(\mathbf{2})_2](PF_6)_2(NO_3)]^{3+}$, and $[[Cu_3(\mathbf{2})_2](NO_3)]^{5+}$ (see Supporting Information, Figure S7). In addition to this series of peaks, other minor peaks are observed that are due to associated acetonitrile molecules (as indicated in Figure 3). One minor peak appears at 434.5 *m*/*z* and is identified as a +3 charged fragment corresponding to the monometallic $\{[Cu(\mathbf{2})(CH_3CN)]^{2+} + H^+\}$species. The major peaks observed in the mass spectrum suggest that in the gas phase the molecular ion $[Cu_3(\mathbf{2})_2]^{6+}$ is most stable with mixed anions and that the NO_3^- anion is associated more tightly. It is possible that given the high charge of the complex, the solution structure similarly contains associated anions and solvent molecules.

Taken together, the VPO, HPLC and mass spectrometry data are consistent with a single supramolecular

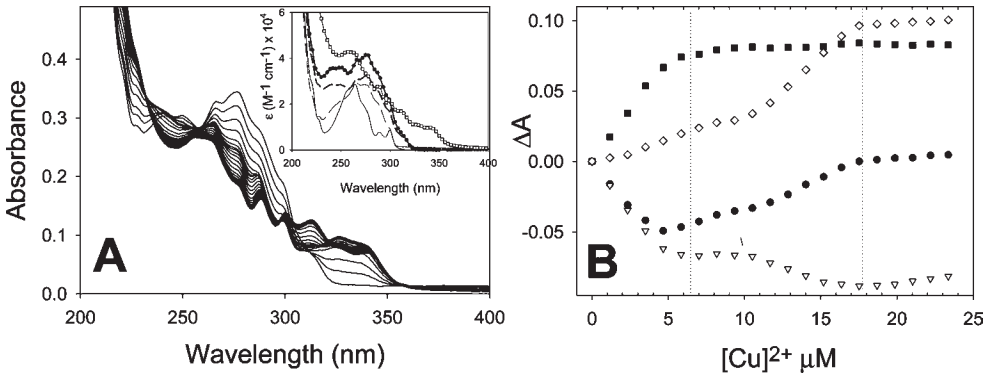

Figure 4. (A) UV−vis absorbance spectra of the titration of 2.0 mL of 7.79 μM tripeptide **2** with 50 μL injections of 38.9 μM $Cu(NO_3)_2$ in methanol. Inset: Extinction spectra of the py monomer (solid line); bpy monomer (− − −); tpy monomer (- - -); tripeptide **2** (-●-); and Cu tripeptide complex $[Cu_3(\mathbf{2})_2](PF_6)_6$ (-□-) in acetonitrile solutions. (B) Titration curves for the addition of Cu^{2+} into 2.0 mL 7.79 μM tripeptide **2**, monitored at 276 nm (▽); 300 nm (●); 313 nm (◇) and 340 nm (■).

complex consisting of three Cu(II) ions and two tripeptides, that is, $[Cu_3(\mathbf{2})_2]^{6+}$. The ^{1}H NMR spectrum of the Cu(II) complex (Supporting Information, Figure S8) reveals severe peak broadening because of the presence of paramagnetic Cu(II), but because of these paramagnetic shifts, demonstrates that all three ligands (py, bpy, and tpy) are coordinated to Cu(II). To coordinatively saturate the three Cu(II) centers with six available ligands on two tripeptide strands, the most likely structure of $[Cu_3(\mathbf{2})_2]^{6+}$ is one in which the chains are oriented antiparallel as in Figure 1B. Although other Cu(II) complexes can form from the pendant ligands, the structure that is consistent with all of the above data is one that contains two $[Cu(tpy)(py)]^{2+}$ and one $[Cu(bpy)_2]^{2+}$ complex cross-links. Obtaining this product, instead of polymers or offset orientations, is most likely driven by entropic factors, similar to observations in molecular rectangles, triangles, boxes, and so forth.[10]

Spectrophotometric Titrations of Tripeptide. The identities of the coordinative cross-links between two tripeptide strands, together with the binding stoichiometry, are evaluated using the UV and visible spectra acquired during titration of the tripeptide with Cu(II). The UV−visible absorbance spectrum of the tripeptide shown in Figure 4 is dominated by strong absorption by the pendant ligands and terminal Fmoc group in the UV region. Fmoc absorbs at wavelengths between 240 and 270 nm, overlapping the py, bpy, and tpy absorption peaks that are due to $\pi-\pi^*$ transitions. The Figure 4A inset compares the measured extinction spectra of the py, bpy, and tpy monomers with the tripeptide; the tripeptide spectrum is not equivalent to a linear sum of the monomers because there is one terminal Fmoc group appended to each of the four species. However, the $\pi-\pi^*$ transition peaks are known to shift to longer wavelengths when metal is coordinated,[15,16] and the extinction spectrum of the Cu(II) complex of the tripeptide (isolated above) shows that the new peaks appear at $\lambda > 310$ nm.

Addition of Cu(II) to the tripeptide during a spectrophotometric titration causes complex changes in the spectrum that are the result of having three different ligands and several possible metal−ligand complexes within the structure (e.g., $[Cu(bpy)]^{2+}$, $[Cu(bpy)_2]^{2+}$; $[Cu(tpy)(bpy)]^{2+}$, etc.). In Figure 4A, titration with Cu(II) results in the appearance of several isosbestic points. When the amount of added Cu(II) is less than 10 μM, isosbestic points appear at 257 and 310 nm; continued addition of Cu(II) results in three new isosbestic points at 231, 297, and 323 nm (Supporting Information, Figure S9). We quantitatively examine changes in absorbance at wavelengths longer than 310 nm because the oligopeptide does not absorb in this region, but new bands appear during the titration. Titration curves generated from these data are shown in Figure 4B and contain inflection points at $[Cu^{2+}] \sim 6.5$ and 18 μM. The first of these is at approximately a 0.8:1 Cu/tripeptide ratio. At this molar ratio, the species formed has an extinction coefficient at 340 nm of 12800 M^{-1} cm^{-1}, comparable to that for $[Cu(tpy)]^{2+}$ and $[Cu(tpy)(py)]^{2+}$ (i.e., 14500 and 12600 M^{-1} cm^{-1}, respectively, as shown in Supporting Information, Figure S10A). There are no significant absorption bands by bpy or py complexes of Cu(II) at wavelengths above 330 nm.[2] The inflection point at low concentrations of added Cu(II) therefore suggests saturation of the available tpy sites; however, we cannot distinguish between formation of $[Cu(tpy)]^{2+}$ and $[Cu(tpy)(py)]^{2+}$. The inflection point observed at 313 nm with 18 μM added Cu(II) is due to formation of a product with extinction coefficient 10870 M^{-1} cm^{-1}. Both $[Cu(bpy)]^{2+}$ and $[Cu(tpy)]^{2+}$ have extinction coefficients consistent with this value, and it is likely that at high concentrations of Cu(II) that the equilibria shift toward these species.[17,18] Additional changes at shorter wavelengths in the spectrum occur during the titration, but because of overlap with absorbance of the unmetalated oligopeptide these cannot be quantitatively analyzed.

The tripeptide does not absorb in the visible region of the spectrum, and combination of tripeptide with Cu(II) causes the growth of a broad absorption band centered at 670 nm, as shown in Figure 5. Initial absorption in this region is typically assigned to the d-d transition of Cu(II); however, the peak that evolves during the titration has a maximum absorbance wavelength that is consistent with a charge transfer band of $[Cu(bpy)_2]^{2+}$ ($\lambda_{max} \sim 700$ nm),

(15) Jorgensen, C. K. *Adv. Chem. Phys.* **1963**, *5*, 33–146.
(16) Sone, K.; Krumholz, P.; Stammreich, H. *J. Am. Chem. Soc.* **1955**, *77*, 777–780.
(17) Yamanchi, O.; Benno, H.; Nakahara, A. *Bull. Chem. Soc. Jpn.* **1973**, *46*, 3458–3462.
(18) Ozutsumi, K.; Kawashima, T. *Inorg. Chim. Acta* **1991**, *180*, 231–238.

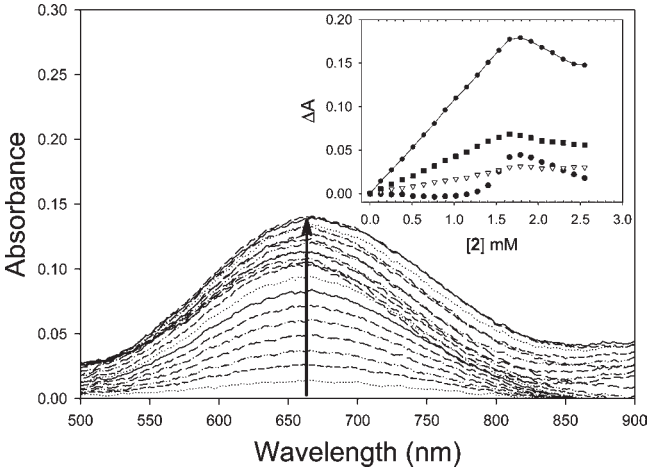

Figure 5. UV−vis absorbance difference spectra of the titration of 9.87 mM tripeptide **2** titrated in 50 μL increments into a 2.0 mL volume of 1.91 mM $Cu(NO_3)_2$ in methanol. Inset: Titration curves during this experiment, monitored at 520 nm (■); 570 nm (▽); 670 nm (-●-); and 900 nm (●).

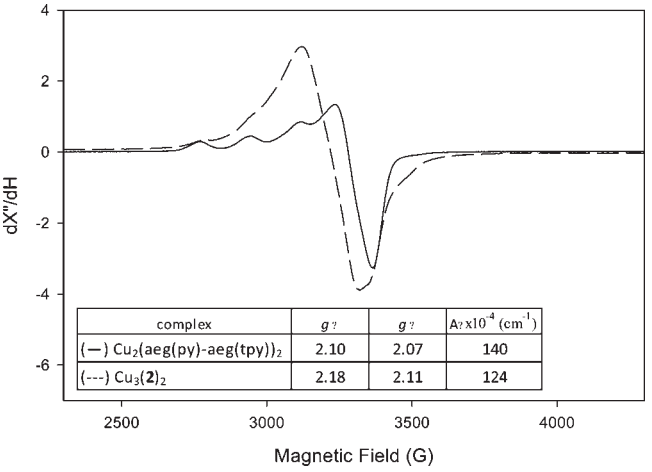

Figure 6. EPR spectra of 1 mM frozen solutions of the two Cu peptide complexes in ACN. Inset: EPR parameters calculated from spectra.

$[Cu(tpy)]^{2+}$ (λ_{max} ~695 nm), and $[Cu(tpy)(py)]^{2+}$(λ_{max} ~650 nm) (see Supporting Information, Figure S10B), so that formation of these cannot be distinguished in the visible region. However, the observed peak maximum is suggestive of a mixture of $[Cu(bpy)_2]^{2+}$ with a geometric distortion to a compressed tetrahedron,[19] because of the steric hindrance between the 3,3′ protons,[20] and $[Cu(tpy)(py)]^{2+}$ with a coplanar geometry.[19]

Given the above experimental data, it is likely in the spectrum in Figure 5 that the λ_{max} of 670 nm is a result of both $[Cu(tpy)(py)]^{2+}$ and $[Cu(bpy)_2]^{2+}$ cross-links. Quantitative analysis of the titration curves was again performed to identify the product(s). The titration curves in the Figure 5 inset monitored at all wavelengths have inflection points at 1.7 mM added tripeptide, which is equivalent to a molar ratio of 1.1:1 Cu (II)/tripeptide **2**. At this stoichiometric point, the calculated extinction coefficient of the product(s) at 670 nm is determined to be 82 M^{-1} cm^{-1}. Because at this wavelength ε for $[Cu(bpy)_2]^{2+}$, $[Cu(tpy)]^{2+}$, and $[Cu(tpy)(py)]^{2+}$ are 95.5, 76.6, and 72.6 M^{-1} cm^{-1}, respectively, the result is consistent with formation of each of these during the titration but cannot distinguish between them. In Supporting Information, Figure S10B, the experimentally measured extinction of the trimetallic tripeptide duplex agrees well with the calculated spectrum of two $[Cu(tpy)(py)]^{2+}$ plus one $[Cu(bpy)_2]^{2+}$, with some deviation at long wavelengths that reflects the geometry of the $[Cu(bpy)_2]^{2+}$.[19]

Electron Paramagnetic Resonance Spectroscopy. Electron paramagnetic resonance (EPR) spectroscopy is used to further confirm the identities of the Cu(II) complex cross-links in the tripeptide duplex, and to investigate the coordination environment of the Cu(II) centers. We hypothesized that the longer oligopeptide strand with three metal ion cross-links would provide a stiffer scaffold (versus a dipeptide duplex with two Cu(II) cross-links) and therefore force greater metal−metal interactions. The measured EPR spectrum of the Cu(II) complex of the tripeptide was therefore compared to that of a dimetallic dipeptide analogue, $[Cu_2(Fmoc\text{-}aeg(py)\text{-}aeg(tpy)\text{-}OtBu)_2](PF_6)_4$.[6d] EPR spectra in frozen acetonitrile solutions were obtained for the two complexes (Figure 6), providing insight into the coupling and local environment of the Cu(II) in each molecule. Comparing the integrated area of the peaks to a Cu(II) standard solution, the spectra in Figure 6 are the result of Cu(II) concentrations of 2.1 and 3.6 mM, consistent with the concentrations of 1.0 mM $[Cu_2(Fmoc\text{-}aeg(py)\text{-}aeg(tpy)\text{-}OtBu)_2](PF_6)_4$ and 1.1 mM $[Cu_3(\mathbf{2})_2]^{6+}$, respectively. Parameters listed in the inset table include values of $g_{\|} > 2.1 > g_{\perp} > 2.0$,[21] suggesting that the lone electrons are in the $d_{x^2-y^2}$ ground state[7] and signifying that the dominant geometry in the metalated tripeptide duplex is square planar.

The difference in line widths of the low-field hyperfine resonances (17.4 mT for $[Cu_2(Fmoc\text{-}aeg(py)\text{-}aeg(tpy)\text{-}OtBu)_2](PF_6)_4$ and 16.5 mT for $[Cu_3(\mathbf{2})_2]^{6+}$) offers initial evidence that the Cu(II) in the two duplexes have different environments. The shape of the spectrum of $[Cu_2(Fmoc\text{-}aeg(py)\text{-}aeg(tpy)\text{-}OtBu)_2](PF_6)_4$ is similar to the spectra of the small molecules ($[Cu(bpy)_2]^{2+}$ and $[Cu(tpy)(py)]^{2+}$, Supporting Information, Figure S11A and B. However, the EPR spectrum of $[Cu_3(\mathbf{2})_2]^{6+}$ is drastically different, and is not equivalent to the linear combination of the spectra of $[Cu(bpy)_2]^{2+}$ and $[Cu(tpy)(py)]^{2+}$ (Supporting Information, Figure S11C). Instead, significant line broadening in the $[Cu_3(\mathbf{2})_2]^{6+}$ spectrum suggests the Cu(II) centers are extensively interacting rather than electronically isolated: because $A_{\|}$ is significantly $< 150 \times 10^{-4}$ cm^{-1}, this hyperfine splitting value suggests coupling between Cu(II) ions in $[Cu_3(\mathbf{2})_2]^{6+}$ as a result of being held closer than 6 Å.[22] Even though tethering the positively charged metal centers close to one another would result in electrostatic repulsion, the EPR spectra clearly demonstrate that extension of the oligopeptide to three monomer units creates a rigid enough scaffold to overcome some of this force. Association with anions may also attenuate electrostatic effects.

(19) Hathaway, B. J. *Struct. Bonding (Berlin)* **1984**, *57*, 55–118.
(20) McKenzie, E. D. *Coord. Chem. Rev.* **1971**, *6*, 187–216.
(21) Wei, N.; Murthy, N. N.; Karlin, K. D. *Inorg. Chem.* **1994**, *33*, 6093–6100.
(22) Solomon, E. I.; Sundaram, U. M.; Machonkin, T. E. *Chem. Rev.* **1996**, *96*, 2563–2605.

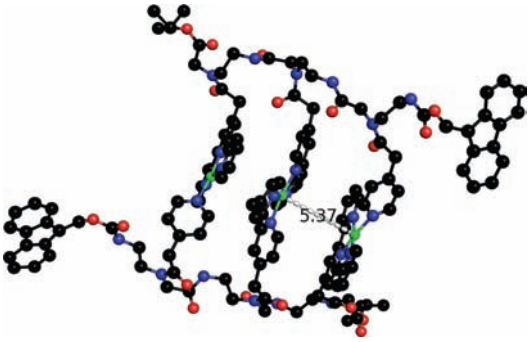

Figure 7. Molecular model calculated with a MM+ force field $[Cu_3(\mathbf{2})_2]^{6+}$, with the Cu(II) centers are shown in green.

Molecular Modeling. In context with all of the available analytical data, the spectrophotometric titrations and EPR spectra provide strong evidence for the formation of a tripeptide duplex linked by three Cu(II) complexes that are two $[Cu(tpy)(py)]^{2+}$ and one $[Cu(bpy)_2]^{2+}$. To visualize the solution structure of the Cu(II)-linked tripeptide duplex, molecular modeling incorporating all of the available characterization information was performed. In Figure 7, a molecular model was generated using a full geometry optimization performed in vacuum using HyperChem (Version 6, HyperCube Inc.) with the MM+ force field. The steepest descent algorithm and a termination condition with a rms gradient of 0.1 kcal mol^{-1} $Å^{-1}$ were employed during the optimization. The resulting tripeptide duplex structure consists of distorted square planar and compressed tetrahedral geometries of the $[Cu(tpy)(py)]^{2+}$ and $[Cu(bpy)_2]^{2+}$ cross-links, respectively. This calculation shows a structure with a metal−metal separation distance of ~5 Å, consistent with the coupling observed in the EPR spectrum, although conformational flexibility in solution potentially makes the separation distance dynamic.

Our continuing efforts aim to identify the appropriate conditions with which these supramolecular structures will form crystallographic quality crystals. The synthetic methodology used to prepare the tripeptide can be applied to prepare longer structures for added rigidity, which may be necessary to drive crystallization. The studies here provide the necessary foundation to enable characterization of the multimetallic structures and use this understanding to apply the molecular design motif and artificial oligopeptides to build supramolecular structures of increasing complexity and function.

Acknowledgment. This work is generously supported by a grant from the National Science Foundation (CHE - 0718373). We thank Prof. Squire Booker and Tyler Grove for their assistance with the EPR measurements.

Supporting Information Available: EPR and NMR spectra, titration spectra at low and high concentrations of Cu(II), and extinction spectra of small molecule components. This material is available free of charge via the Internet at http://pubs.acs.org.